

1
2
3
4
5
6
7
8
9
10
11
12
13
14
15
16
17
18
19
20
21
22
23
24
25

26
27
28
29
30
31
32
33

34
35

Mediterranean Warm-Core Cyclones in a Warmer World

Kevin Walsh
School of Earth Sciences
University of Melbourne

Filippo Giorgi, Erika Coppola
International Centre for Theoretical Physics, Trieste

For submission to Climate Dynamics
October 4, 2012
Revised January 27, 2013

Corresponding author: Kevin Walsh, School of Earth Sciences, University of Melbourne
3010 Victoria Australia. e-mail: kevin.walsh@unimelb.edu.au

36

37 **Abstract**

38

39

40

41 Regional climate model projections over the Mediterranean region are analysed for the
42 presence of intense, warm-core lows that share some of the characteristics of tropical
43 cyclones. The results indicate that the number of such systems decreases in a warmer world,
44 particularly in winter. Comparison of the simulated numbers to changes in relevant climate
45 diagnostics suggests that numbers decrease due to an increasingly hostile environment for
46 storm formation, combined with a general poleward shift in the incidence of wintertime lows
47 over western Europe.

48

49 **1. Introduction**

50
51

52 It has been previously shown that some storms forming and developing in the Mediterranean
53 Sea have some of the structural characteristics of tropical cyclones (e.g. Reale and Atlas
54 2001; Emanuel 2005). Numerous studies have shown that tropical cyclones differ from
55 baroclinically-forced systems in that they are warm core systems whereas extratropical
56 cyclones usually are cold cored (Haurwitz 1935; Mayengon 1984). More recently, attention
57 has focused on a subset of intense, small Mediterranean warm-core systems, popularly known
58 as “medicanes”, with a number of studies examining their structure and characteristics
59 (Lagouvardos et al. 1999; Pytharoulis et al. 2000; Fita et al. 2007; Tous et al. 2010; Tous and
60 Romero 2011, 2012). Typically, the rate of occurrence of these storms in the Mediterranean
61 basin is less than one per year.

62

63 The recent study of Tous and Romero (2012) thoroughly characterizes the synoptic
64 environment of these rare storms. A database of events is compiled using a combination of
65 automated and manual detection techniques and their typical formation conditions are
66 elucidated through the comparison of a number of diagnostics. Medicane formation is
67 associated with high diabatic heating from surface fluxes, sea surface temperatures (SSTs)
68 greater than 15 degrees C and larger than normal values of Maximum Potential Intensity
69 (MPI; Bister and Emanuel 1998), a diagnostic more usually associated with tropical cyclone
70 intensity.

71

72 In general, because of the small size of these storms (a diameter of less than 300 km), they
73 have been poorly simulated in climate models. A recent exception is the high-resolution
74 simulations of Cavicchia and von Storch (2012). Using resolutions as fine as 10 km, they
75 were able to simulate successfully the generation of medicane cases described in the literature

76 when the model was initialised two weeks in advance of storm formation. Since this time
77 period is long enough so that the model's simulation of short timescale phenomena such as
78 medicanes was no longer sensitive to initialization, this study demonstrated the potential of
79 this modeling approach to generate medicanes when running in climate mode.

80

81 Previous climate model simulations have suggested that deep Mediterranean low pressure
82 systems may become more intense or more numerous in a warmer world. For example,
83 Gaertner et al. (2007) analysed results from the regional climate model (RCM) simulations
84 generated as part of the PRUDENCE project (Christensen et al. 2002). These simulations
85 were performed at a horizontal resolution of 50 km and were forced by a suite of general
86 circulation models (GCMs). The results showed a wide range of responses across RCMs, but
87 in general the frequency of cyclone centres increased in a warmer world, accompanied by
88 increases in the 95th percentile of storm intensity, as measured by the low-level geostrophic
89 vorticity. Gaertner et al. (2007) also investigated the structural characteristics of
90 Mediterranean lows, particularly the limited subset of lows that have clear warm-core
91 characteristics, as deduced from the phase-space diagram of Hart (2003). The changes of
92 these storms in a warmer world were model-dependent, with some models showing increases
93 in storm lifetimes while others did not.

94

95 In further work, Gaertner et al. (2011) employed a similar methodology to analyse the results
96 of the ENSEMBLES project (Hewitt and Griggs 2004), a suite of RCM simulations at 25 km
97 resolution. They used the tropical cyclone detection method of Picornell et al. (2001) to
98 detect intense warm core lows over the Mediterranean, of which true medicanes would be a
99 subset. They concluded that for most simulations, the number of storms in the Mediterranean
100 was reduced in a warmer world but their intensity was slightly increased. Lionello et al.

101 (2008) also analysed changes in the frequency and intensity of cyclones in regional climate
102 change projections with a horizontal resolution of 50 km over the European region and found
103 a predominant decrease of the frequency of storms over the Mediterranean region, but more
104 contrasting results concerning changes in peak storm intensity. Clearly, further work is
105 needed in order to assess more firmly possible changes in frequency and intensity of
106 Mediterranean storms under global warming conditions.

107

108 In the present study we complement previous work by focusing on a subset of all
109 Mediterranean lows, those that have high wind speeds and warm cores. Throughout the paper
110 we refer to such storms as “warm core lows”. A further subset of these, consisting of small,
111 intense, symmetric storms, is considered in the present study to have characteristics similar to
112 those of observed medicanes. To complement the work of Gaertner et al. (2011), we also
113 examine changes in the incidence of all intense lows, not just warm core systems, and use
114 relevant diagnostics to examine changes in the physical factors that are related to storm
115 formation. We analyze RCM simulations of present day and future climate conditions under
116 increased greenhouse gas concentrations over the European region to determine the response
117 of simulated warm core lows to anthropogenic climate change, and to examine the
118 geographical variation of this response. We accomplish this goal by using a storm detection
119 and tracking algorithm specifically designed to identify warm core systems. Section 2 of the
120 paper details the methodology, Section 3 gives results and Section 4 provides a discussion
121 and concluding remarks.

122

123 **2. Methodology**

124 The simulations analysed here are from the regional model RegCM3 (Giorgi et al., 1993a,b;
125 Pal et al. 2007) running at a horizontal grid spacing of 25 km and 18 sigma-p vertical levels.

126 The model employs the radiative transfer scheme of Kiehl et al. (1996), a non-local planetary
127 boundary parameterization based on Holtslag et al. (1990), the Biosphere-Atmosphere
128 Transfer Scheme (BATS, Dickinson et al. 1993) for the description of land surface processes,
129 the cumulus convection scheme of Grell (1993) and the resolvable precipitation
130 representation of Pal et al. (2000).

131

132 These simulations were performed as part of the ENSEMBLES project (Hewitt and Griggs
133 2004) and in particular two experiments are considered here. The first uses lateral boundary
134 conditions from the ERA40 reanalysis (Uppala et al. 2005), while the second is driven by
135 output from a scenario simulation conducted with the ECHAM5 general circulation model
136 (Roeckner et al. 2003). The scenario simulation extends from 1951 to 2100 under greenhouse
137 gas forcing from the A1B emission scenario of Nakicenovic and Swart (2000) and we
138 analyze here three time slices: 1981-2000 for current climate and 2041-2060, 2081-2100 for
139 future climate conditions.

140

141 The model output is then analyzed to test the model's ability to generate intense low pressure
142 systems in the Mediterranean. Intense Mediterranean lows are detected using the CSIRO
143 tropical cyclone detection scheme of Walsh et al. (2004). The steps used by this detection
144 routine are as follows:

145

146 • Points with cyclonic vorticity greater than $1 \times 10^{-5} \text{ s}^{-1}$ are first identified; this
147 threshold serves only to eliminate isolated points of weak cyclonic vorticity,
148 thus speeding up the detection routine (the actual intensity threshold is set by
149 the wind speed criterion below);

150 • A centre of low pressure is then found;

- 151 • At the centre of the storm a warm core is found, specified as the sum of the
152 temperature anomalies at the storm centre versus the surrounding
153 environment, with the temperature anomaly at 300 hPa being greater than
154 zero; in addition, the mean wind speed over a specified region at 850 hPa must
155 be greater than that at 300 hPa.
- 156 • A minimum 10 m wind speed threshold of 17.5 ms^{-1} is then imposed, such that
157 wind speeds within the storm must exceed this value; this corresponds to the
158 observed defined threshold of tropical storm strength

159 Detections of very small, intense warm-core lows were also compared with the observed
160 medicane cases of Tous et al. (2011) and Tous and Romero (2012) to determine the ability of
161 the model to generate these rare Mediterranean storms. In order to estimate future changes in
162 storm characteristics, storm statistics in the future time slices of the ECHAM-driven run were
163 compared to the corresponding values in the current climate period.

164

165 The detection scheme produces storms tracks, including storm intensity, that are then
166 analysed to produce genesis density and track density plots, in number of storm formations or
167 tracks per 2×2 degree grid square. Like all such schemes, one of its main limitations is the
168 possibility that the tracking may not be entirely consistent between storms, leaving gaps in
169 the tracks along with possible double-counting of storms. This possibility is excluded by
170 manual inspection of the resulting storm tracks. Compared with other widely-used storm
171 tracking schemes (e.g. Murray and Simmonds 1991a,b; Flocas et al. 2010), this scheme has
172 the advantage of simplicity and is well suited to the detection of rare events such as warm-
173 core Mediterranean lows.

174

175 **3. Results**

176 3.1. Simulated storm numbers

177

178 Figure 1 shows results for the detection of intense warm-core systems in the simulation
179 nested within the ERA-40 reanalysis, for both the full year and seasonally varying conditions.
180 A storm is detected if it occurs once in the data set (which is archived four times a day) and
181 numbers are summed over 2x2 degree grid squares. Thus one detection corresponds to a
182 single detection in that grid square over the period of simulation, in this case 1981-2000. The
183 plots are then smoothed to reduce random spatial variability between grid squares. Figure 1
184 shows that these systems are generally infrequent. A strong seasonal variation in the
185 simulation of intense storms is simulated, with considerably more occurring in the winter
186 months than in the summer. Maximum occurrence in the winter season is in the western
187 Mediterranean to the west of Sardinia, but other important regions of occurrence are located
188 over the Adriatic Sea southern Italy and in the Aegean. A number of such storms are also
189 generated in the Black Sea (Efimov et al. 2008). A similar pattern is seen in the climatology
190 of Maheras et al. (2001), derived from NCEP reanalysis (Kistler et al. 2001). Fig. 2 shows
191 the Maheras et al. (2001) winter climatology of intense storms, defined as those with central
192 pressures less than 995 hPa. They showed a similar strong seasonal dependence in their
193 observational analysis to that shown in Fig. 1: essentially no such storms are observed in the
194 summer over the Mediterranean and the Black Sea, while a pronounced winter maximum is
195 seen. Fig. 2 shows that geographical maxima of winter storm occurrence in the observations
196 are located over the Gulf of Genoa, the northern Adriatic, and over southern Greece (Maheras
197 et al. 2001; their Fig. 6f). In the observations of Maheras et al. (2001) there is also a tongue of
198 high observed occurrence running north from the north-central Black Sea region into Ukraine
199 and Russia. This is also simulated by RegCM3, as shown in Fig. 1.

200

201 Fig. 1 also shows that a large number of such intense, warm-core storms are also simulated
202 off the west coast of western Europe and over the British Isles. It is possible that such storms
203 are examples of the subset of extratropical systems that evolve in a manner consistent with
204 the warm seclusion mechanism proposed by Shapiro and Keyser (1990), where extratropical
205 storms can possess a warm core during part of their lifecycles. This hypothesis is difficult to
206 confirm without significant additional analysis. In any event, our focus in this study is on the
207 Mediterranean region.

208

209 An analysis was also undertaken of these simulated lows to determine whether the
210 simulations were generating the observed lows within the interior of the domain, rather than
211 simply generating a similar statistical distribution of such systems with no day-to-day
212 correspondence between simulated and observed lows. A manual examination of the forcing
213 ERA-40 reanalyses showed that almost all of the detected lows in the ERA-40 RegCM3
214 simulations shown in Fig. 1 were also observed in the forcing ERA-40 reanalyses, at similar
215 locations. This implies that the model is able to reproduce a representative set of real
216 Mediterranean low pressure systems.

217

218 In contrast, very few of the observed medicane cases of Tous et al. (2011) or Tous and
219 Romero (2012) can be seen in the model simulations forced by reanalyses. Clearly, for such
220 small systems, stochastic formation processes must dominate, thus leading to a poor
221 simulation of their observed formation in a model experiment like this one that is run in
222 climate mode without reinitialisation. There is one exception: the medicane of late October
223 1994 that formed to the southeast of Sicily. This appears to be well simulated by RegCM3
224 when forced by ERA-40. Fig. 3 shows the simulated mean sea level pressure of this case,
225 while Fig. 4 shows the simulated warm core anomaly, here defined as the sum of the mid-

226 tropospheric temperature anomalies versus the surrounding temperatures at those levels. The
227 storm is small, has a strong warm core and clearly shares a number of the defined
228 characteristics of a medicane. Tous et al. (2011) and Tous and Romero (2012) define these
229 largely from the storm's appearance in satellite images: a diameter less than 300 km, the
230 existence of a definite eye, a symmetric and continuous cloud structure surrounding the eye
231 and a duration longer than 6 hours. The storm shown in Figs. 3 and 4 has a diameter less than
232 300 km, appears symmetric and lasted for more than 6 hours. It is noted, however, that the
233 October 1994 storm does not appear in the updated medicane list of Tous and Romero (2012)
234 (their Table 1).

235

236 In this analysis, we define “medicane-like” in a similar fashion to the work of Tous and
237 Romero (2012), although without their analysis of the cloud structure of the storms. Here we
238 define a simulated storm as “medicane-like” if it satisfies the detection conditions listed in
239 section 2, and in addition has a distance of less than three degrees of latitude from its centre
240 to its last closed isobar, appears symmetrical in shape and is located only over the ocean. Of
241 the simulated warm-core systems in the run driven by ERA-40 reanalyses, a subset of these
242 appear to have the characteristics of medicanes, even though apart from the October 1994
243 storm mentioned above they did not correspond to specific observed medicanes in the
244 available observations. Overall, sixteen “medicane-like” storms were identified in this 20-
245 year period analysed from this run, a similar formation rate to that observed. Their general
246 geographical pattern of occurrence (not shown) indicates a tendency for formation further
247 south than that of other warm-core cyclones, as shown by Tous and Romero (2012). Their
248 seasonal variation shows a maximum in winter, instead of the autumn maximum shown by
249 Tous and Romero (2012), thus indicating a possible inclusion of other warm core systems in
250 our definition, as these have a clear maximum in winter.

251 Some further analysis was performed to determine whether the formulation of the detection
252 routine was causing simulated medicanes not to be detected, through the imposition of
253 unnecessarily strict detection criteria. Another detection run was performed, this time turning
254 off the requirement for a warm core, and a similar search for medicane-like storms was made.
255 The results (not shown) did not represent a substantial improvement in the simulation of the
256 observed Tous and Romero (2012) medicane cases, suggesting that initialization issues are
257 critical in generating these small storms in the correct locations.

258

259 We have examined the changes in medicane numbers in the ECHAM5-driven simulations in
260 the current and future climates. A total of 19 medicane cases were identified in the current-
261 climate simulation, while this number decreased to 8 in the 2081-2100 simulations. Thus
262 there is a clear decrease in medicane-like storm numbers. We also examined any changes in
263 the intensity distribution of these storms in a warmer world, but since numbers are low, it was
264 difficult to draw any conclusions. Since the number of true medicane cases appears to be
265 small, both in the observations and the simulations, and their identification in the simulations
266 has a subjective component, we instead focus on the larger group of warm-core cyclones for
267 subsequent analysis.

268

269 The comparison of Fig. 1 to the regional model simulation nested with the current-climate
270 output from the ECHAM5 model is instructive. Figs. 5 and 6 show that the patterns of
271 occurrence when the regional model is nested within the reanalysis and the GCM are similar,
272 but the number of storms generated by the GCM nesting is somewhat larger. Figure 6 shows
273 that the ECHAM5 run has more pronounced maxima over the Black Sea, the Italian
274 peninsula and the Bay of Biscay, and to a lesser extent over the Aegean, in regions
275 corresponding to maximum cyclone occurrence in both runs. Examination of the surface

276 temperature fields in the ERA40 and ECHAM5 runs shows that the surface temperature in
277 the ECHAM5 run is slightly colder over the Mediterranean and the meridional temperature
278 low-level gradient is slightly greater over the northern Mediterranean in the ECHAM5 run.
279 This suggests a relationship between this increased gradient and the larger number of storms
280 in this run.

281

282 The climate change simulation of the ECHAM5-nested runs was next examined. Fig. 7 shows
283 the differences in numbers of lows from the current climate simulation for the period 2041-
284 2060 and 2081-2100. The patterns of differences in the two time periods are remarkably
285 similar: in January-March, for both time periods there are decreases in numbers in the region
286 near Sardinia and increases over the Gulf of Genoa and northern Italy. Both time periods also
287 show decreases over southern Greece and the central Black Sea region, as well as the Bay of
288 Biscay. The consistency of this response across two separate time periods suggests that it is
289 systematic and not a result of multidecadal variability. Due to the similarity of the response in
290 the two time periods, we will focus on results for the later period of 2081-2100.

291

292 Total numbers of intense storms over the Mediterranean region decrease in a warmer world,
293 however. Figure 8 shows intensity distributions of storm maximum wind speeds over the
294 Mediterranean region bounded by 5-40E, 30-45N. As the climate is projected forward in
295 time, the total numbers of storms drop but the maximum wind speed reached in each time
296 period increases. Few storms exceed hurricane intensity (33 ms^{-1}), however.

297

298 3.2 Climate diagnostics

299

300 *Maximum potential intensity*

301

302 A useful diagnostic for understanding the intensification of tropical cyclones is the
303 Maximum Potential Intensity (MPI; Bister and Emanuel 1998). Since we are examining here
304 the small subset of intense Mediterranean cyclones that have significant warm cores, it is of
305 interest to determine whether the MPI diagnostic can give insight into the simulated changes
306 in cyclone characteristics. We focus on the JFM season as this is the season with the most
307 cyclones and we show maximum low level wind speed (V_{max}) calculated from the MPI
308 theory. Comparing Figures 9(a) and Figure 8(a), we see that V_{max} is in generally agreement
309 with the maximum intensity of the simulated storms, with highest intensities between 25 and
310 30 ms^{-1} . By 2081-2100, Figure 9(b) gives decreases in V_{max} over the Mediterranean mostly
311 between 2 and 5 ms^{-1} . In contrast, Figure 8(b) shows that the maximum intensity of the
312 strongest storms increases, although there are a only few storms that exceed 30 ms^{-1} in
313 intensity. The total number of intense storms decreases in the warmer world simulations, and
314 this may be a more accurate reflection of the impact of decreasing V_{max} .

315

316

317 *Vertical wind shear*

318

319 Warm-core systems, both tropical and subtropical cyclones, can be disrupted or prevented
320 from forming by vertical wind shear, the magnitude of the vector difference between winds in
321 the upper and lower troposphere (e.g. Briegel and Frank 1987). Vertical wind shear V_z is
322 defined here as

323

324

325 where the zonal and meridional velocities are evaluated at 300 and 850 hPa. Figure 10 shows
326 the change in vertical winds shear for JFM. Climatological wind shear is significantly greater
327 in the warmer world simulation, with a substantial area of the Mediterranean having average
328 wind shears more than 4 ms^{-1} greater. This climatological average difference is large enough
329 to affect the generation rate of tropical cyclones (e.g. Shapiro 1987) and may have some
330 relevance in possibly inhibiting the future formation of cyclones in our scenario simulation.

331

332 *Eady growth rate*

333

334 The Mediterranean is located in a region subject to baroclinic processes. A standard measure
335 of the intensity of baroclinicity is the Eady growth rate (EGR; Eady 1949; Vallis 2006):

336

$$\frac{f}{N^2} \frac{dU}{dz}$$

337

338 where N is the Brunt-Väisälä frequency, f is the Coriolis parameter and U is the zonal wind.

339 Here we diagnose this quantity for current and future climate conditions from mean climate

340 fields. It has been noted by previous authors (e.g. Simmonds and Lim 2009) that it is more

341 accurate to derive the EGR from instantaneous fields and then average to create a

342 climatology. Thus the present, time-mean average diagnostic is intended only as an estimate

343 of whether changes in EGR are consistent in sign with the simulated storm response.

344 Figure 11 shows the difference in EGR for JFM between the current and future climate time

345 periods, for both 600 hPa and 850 hPa heights. Both are given as it is not yet established

346 which of these is most suitable for the assessment of baroclinic conditions (Simmonds and

347 Lim 2009). Simulated 600 hPa EGR (Fig. 11a) in the current climate over the Mediterranean

348 generally increases from west to east, reaching maximum values of between 0.6 and 0.8 day⁻¹
349 over the eastern Mediterranean, similar to observed values for this region derived from
350 reanalyses by Paciorek et al. (2002). Changes in EGR in a warmer world at both levels are
351 generally small (Figs. 11b and d), with slight increases at 850 hPa in the eastern
352 Mediterranean and slight decreases in the west, while there are more uniform but generally
353 small increases at 600 hPa. Since the total number of intense warm-core lows decreases
354 substantially in a warmer world, the small changes in the EGR indicate that baroclinic
355 processes are not a strong contributing factor to the processes driving that change.

356

357 *Comparison between warm core storms and all intense storms*

358

359 The present study focuses on a subset of all Mediterranean cyclones, those with maximum
360 wind speeds comparable to tropical cyclones and with accompanying warm cores. These
361 storms are infrequent, so it is useful to compare the results for this set of storms to a similar
362 set of intense storms with same wind-speed threshold but that do not satisfy the warm-core
363 criterion (Fig. 12a). Comparing Fig. 12a to the observations (Fig. 2), the patterns of formation
364 are quite similar, with largest values over the Italian peninsula and declining towards the east.
365 Comparing Fig. 12a to Fig. 5, we see that the patterns are similar, although the regions of
366 maximum occurrence of the warm core systems appear to be further out into the
367 Mediterranean Sea than those for all intense storms. The difference pattern between current
368 and future climate for all intense storms (Fig. 12b) is similar to that for warm core storms
369 (Fig. 7b), but the differences for the warm-core storms appear more pronounced over the sea
370 than over land. In addition, Fig. 12b appears to show a poleward movement in the incidence
371 of such storms, with increasing numbers over continental regions north of the Mediterranean.

372

373

374 **4. Discussion and conclusions**

375

376 In common with previous work, the results here show that the numbers of Mediterranean
377 cyclones are likely to decrease in a warmer world, for both warm-core and other lows,
378 particularly in winter. A wintertime decrease in numbers of Mediterranean lows is consistent
379 with predictions of a poleward movement of the mid-latitude storm track (e.g. Ulbrich and
380 Christoph 1999; Lionello et al. 2008; Giorgi and Coppola, 2007).

381

382 The new, finer-resolution simulations presented here provide an opportunity to examine the
383 issue of how smaller, intense storms respond to a changed climate. These wintertime
384 decreases are accompanied by a general increase in vertical wind shear over the Basin, some
385 decreases in theoretical tropical cyclone potential intensity, and little change in baroclinic
386 growth rates. An increase in vertical wind shear is well known to affect both tropical and
387 subtropical storm formation rates (e.g. Pezza and Simmonds 2005). Tous and Romero (2012)
388 showed that observed intense cyclones and medicanes in general will not form in very high
389 shear environments, so an increase in climatological shear such as that simulated here would
390 be likely to cause more hostile environmental conditions for these storms.

391 Tous and Romero (2012) also showed that intense Mediterranean lows and medicanes require
392 reasonably high values of MPI to form. The decrease in the climatological value of MPI
393 simulated here would be likely to make it more difficult to form such storms in a warmer
394 world. This is an additional factor that may be related to the simulated future decline in
395 intense warm-core storm numbers shown here.

396 A limitation of the analysis shown here is whether the detection routine is identifying the
397 appropriate subset of intense storms in this region. The detection routine was designed to

398 detect tropical cyclones and has been applied to these simulations without modification.

399 While a number of candidate storms have been detected, it may be that a modification of the

400 warm-core criterion could lead to a better discrimination between storms that are primarily

401 baroclinically-driven and those that derive substantial energy from the sea surface through

402 low-level diabatic heating (Tous and Romero 2012). In addition, even though these

403 simulations have been performed at the highest resolution used to date to simulate the climate

404 of the entire Mediterranean basin, the 25 km resolution used here may still not capture

405 highest intensities of the warm-core mid-latitude storms analysed here, and may not be high

406 enough to effectively capture true medicanes (Cavicchia and von Storch 2012). Since these

407 storms are at least partially convectively-driven, this makes the use of finer horizontal and

408 vertical resolution preferable to best represent these processes. Also, comparison with other

409 simulations would be useful to determine whether these results are robust between models.

410 Fig. 8 shows that while the total number of intense storms decreases, there is a tendency for

411 an increase in the storm maximum intensity. The number of very intense storms with wind

412 speeds greater than 30 ms^{-1} in the future climate run is very small, however.

413 Other limitations of this study are related to the use of a regional climate model and issues of

414 domain specification. A number of studies have shown that the ability of an RCM to simulate

415 a particular atmospheric phenomenon may depend on the exact specification of the domain.

416 For instance, Landman et al. (2005) showed that it was necessary to position the eastern

417 boundary of their domain far enough east so that sufficient tropical disturbances could enter

418 the domain and thus provide a good simulation of tropical cyclone formation. Thus in the

419 regions surrounding the Mediterranean, smaller-scale phenomena that provide initiating

420 mechanisms for some Mediterranean storm systems may not be well represented. Existing

421 larger-scale teleconnection patterns may also be less reliably simulated due to this issue.

422 Phenomena that may be less well represented as a result include interactions between the Red

423 Sea trough and autumn cyclogenesis in the eastern Mediterranean (Ziv et al. 2005) and
424 interactions between tropical African systems and cyclone formation in this region (e.g.
425 Lavaysse et al. 2010, Schepanski and Knippertz 2011). While this issue has not been
426 examined in this study, it is possible that the effects of a warmer climate on tropical systems
427 may have an impact on Mediterranean cyclone formation that could be less well captured in
428 this modeling system.

429

430 A further limitation of this study is associated with the horizontal resolution of the models
431 runs shown here. Cavicchia and von Storch (2012) found that while runs with a horizontal
432 resolution of 25 km gave a good representation of medicane occurrence, maximum wind
433 speeds at such a resolution gave an underestimate of observed wind speeds by 10-30%. A
434 resolution of 10 km was required to best simulate these storms. This restriction would be less
435 of an issue for the larger, warm-core cyclones that we have focused on in this study, however.

436

437 An overarching issue is how well the model simulates the details of the mechanisms of
438 formation of observed cyclones. As Campins et al. (2010) note, the most important formation
439 mechanisms of Mediterranean cyclones of various types are orography, baroclinicity, sensible
440 heat fluxes, latent heat release and upper-level precursor troughs. The limitations of the
441 horizontal and vertical resolution of the model used here will affect each of these
442 mechanisms. For instance, the model may not have sufficient vertical resolution to resolve
443 the upper-level jet instability processes that have been proposed as a genesis mechanism for
444 tropical-cyclone like vortices in this region (Reale and Atlas 2001).

445 In summary, it is found that future projections of intense low pressure systems over the
446 Mediterranean region indicate decreases in the numbers of such systems, particularly in
447 winter. These decreases may be related to a general worsening of the environmental
448 conditions associated with such storms, coupled with a general poleward movement of the
449 typical incidence of such storms.

450

451 **Acknowledgements:** the first author would like to thank the University of Melbourne and
452 ICTP, which both provided partial funding for his visit to ICTP in October-December 2010.
453 The authors would also like to thank the Commonwealth Scientific and Industrial Research
454 Organisation (CSIRO) for the use of their tropical cyclone tracking scheme.

455

456 **References**

457

458 Bister M, Emanuel K (1998) Dissipative heating and hurricane intensity. *Meteorology and*
459 *Atmospheric Physics* 50: 233–240

460

461 Briegel LM, Frank WM (1997) Large-scale influences on tropical cyclogenesis in the western
462 North Pacific. *Mon Wea Rev* 125:1397-1413

463

464 Campins J, Genoves A, Picornell MA, Jansa A (2010) Climatology of Mediterranean
465 cyclones using the ERA-40 dataset. *Int J Climatol* 31: 1596-1614

466

467 Cavicchia L, von Storch H (2012) The simulation of medicanes in a high-resolution regional
468 climate model. *Clim Dyn* (in press).

469

470 Christensen J, Carter T, Giorgi F (2002) PRUDENCE employs new methods to assess
471 European climate change. *EOS* 83: 147

472

473 Dickinson RE, Henderson-Sellers A, Kennedy PJ (1993) Biosphere-Atmosphere Transfer
474 Scheme (BATS) version 1E as coupled to the NCAR Community Climate Model. NCAR
475 Tech. rep. TN-387+STR, 72 p

476

477 Eady ET (1949) Long waves and cyclone waves. *Tellus* 1: 33–52.

478

479 Efimov VV, Stanichnyi SV, Shokurov MV, Yarovaya DA (2008) Observations of a quasi-
480 tropical cyclone over the Black Sea. *Russian Meteorol Hydro* 33: 233–23

481

482 Emanuel K (2005) Genesis and maintenance of Mediterranean hurricanes. *Adv Geosci* 2:
483 217– 220

484

485 Fita L, Romero R, Luque A, Emanuel K, Ramis C (2007) Analysis of the environments of
486 seven Mediterranean storms using an axisymmetric, nonhydrostatic cloud model. *Nat*
487 *Hazards Earth Syst Sci* 7: 41–56

488

489 Flocas HA, Simmonds I, Kouroutzoglou J, Keay K, Hatzaki M, Bricolas V, Demosthenes A
490 (2010) On cyclonic tracks over the eastern Mediterranean. *J Climate* 23: 5243–5257

491

492 Gaertner MA, Jacob D, Gil V, Dominguez M, Padorno E, Sanchez E, Castro M (2007)
493 Tropical cyclones over the Mediterranean Sea in climate change simulations. *Geophys Res*
494 *Letters* 34: doi:10.1029/2007GL029977.

495

496 Gaertner MA, Gil V, Romera R, Domínguez M, Sánchez E, Gallardo C (2011) Climate
497 change scenarios and risk of tropical cyclones over the Mediterranean Sea: analysis with
498 ENSEMBLES data. Presented at the 3rd International Summit on Hurricanes and Climate
499 Change, June 27-July 2, 2011, Rhodes.

500

501 Giorgi F, Marinucci MR, Bates GT (1993a) Development of a second generation regional
502 climate model (REGCM2). Part I: Boundary layer and radiative transfer processes. *Mon Wea*
503 *Rev* 121: 2794-2813.

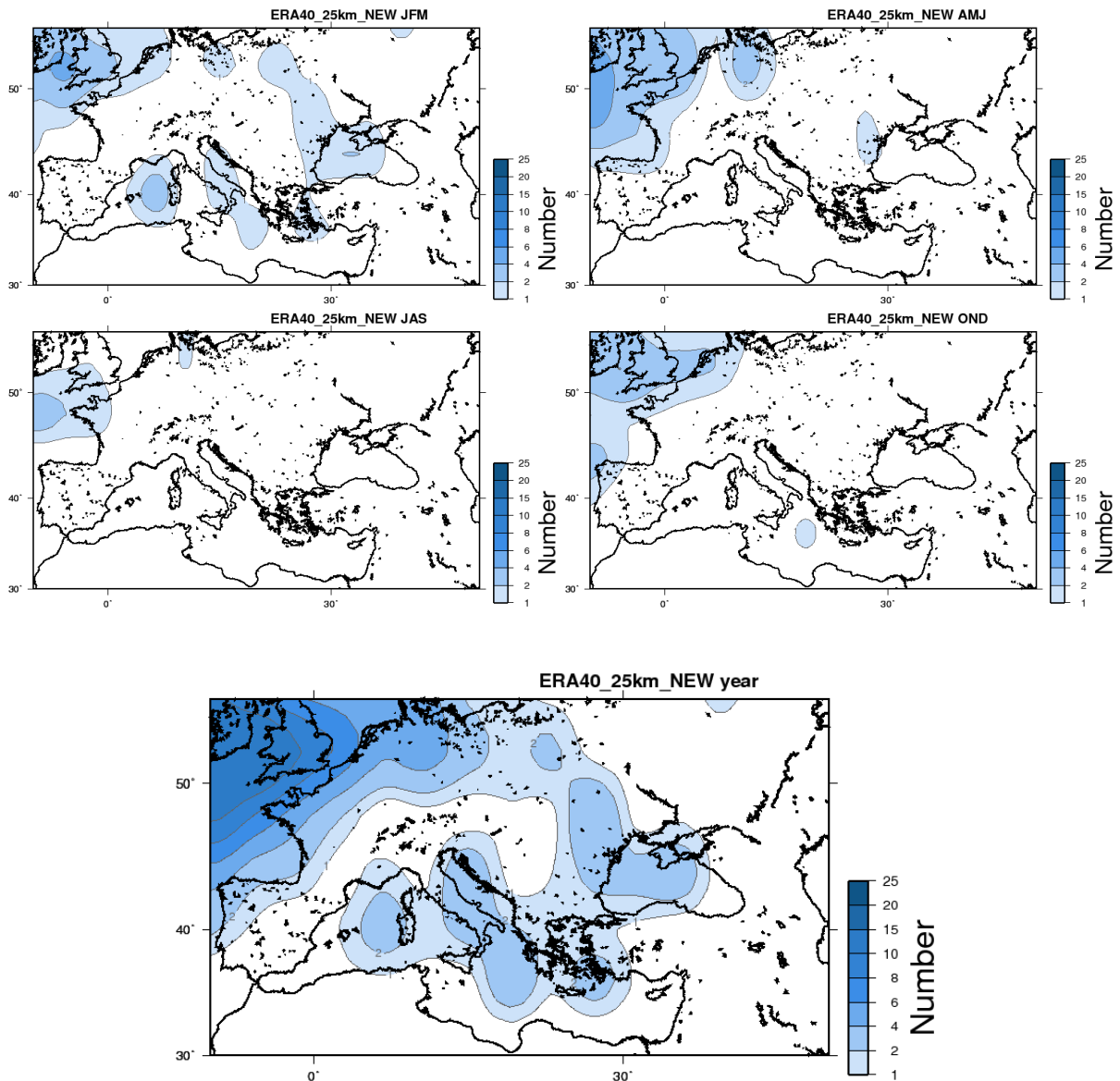
504

- 505 Giorgi F, Marinucci MR, Bates GT, DeCanio G (1993b) Development of a second generation
506 regional climate model (REGCM2). Part II: Convective processes and assimilation of lateral
507 boundary conditions. *Mon Wea Rev* 121: 2814-2832
508
- 509 Giorgi F, Coppola E (2007) European Climate-change Oscillation (ECO). *Geophys Res*
510 *Letters* 34: L21703
511
- 512 Grell GA (1993) Prognostic evaluation of assumptions used by cumulus parameterizations.
513 *Mon Wea Rev* 121: 764–787
514
- 515 Hart R (2003) A cyclone phase space derived from thermal wind and thermal asymmetry.
516 *Mon Wea Rev* 131: 585– 616
517
- 518 Haurwitz B (1935) The height of tropical cyclones and the eye of the storm. *Mon Wea Rev*
519 63: 45-49
520
- 521 Hewitt CD, Griggs DJ (2004) Ensembles-based predictions of climate changes and their
522 impacts. *EOS* 85: 566
523
- 524 Holtslag AAM, de Bruijn EIF, Pan HL (1990) A high resolution air mass transformation
525 model for short-range weather forecasting. *Mon Wea Rev* 118: 1561–1575
526
- 527 Kiehl JT, Hack JJ, Bonan GB, Boville BA, Briegleb BP, Williamson DL, Rasch PJ (1996)
528 Description of the NCAR Community Climate Model (CCM3). NCAR Tech. Rep. TN-
529 420+STR, 152 p
530
- 531 Kistler K, Kalnay E, Collins W, Saha S, White G, Woollen J, Chelliah M, Ebisuzaki W,
532 Kanamitsu M, Kousky V, van den Dool H, Jenne R, Fiorino M (2001) The NCEP–NCAR 50-
533 year reanalysis: monthly means CD-ROM and documentation. *Bull Amer Meteorol Soc* 82:
534 247-267
535
- 536 Lagouvardos K, Kotroni V, Nickovic S, Jovic D, Kallos G, Tremback CJ (1999)
537 Observations and model simulations of a winter sub-synoptic vortex over the central
538 Mediterranean. *Meteorol Appl* 6: 371–383
539
- 540 Landman WA, Seth A, Camargo SJ (2005) The effect of regional climate model domain
541 choice on the simulation of tropical cyclone-like vortices in the southwestern Indian Ocean. *J*
542 *Clim* 18: 1263–1274
543
- 544 Lavaysse C, Flamant C, Janicot S, Knippertz P (2010) Links between African easterly waves,
545 midlatitude circulation and intraseasonal pulsations of the West African heat low. *Quart J*
546 *Roy Meteorol Soc* 136: 141-158
547
- 548 Lionello P, Boldrin U, Giorgi F (2008) Future changes in cyclone climatology over Europe as
549 inferred from a regional climate simulation. *Clim Dyn* 30:657–671
550
- 551 Maheras, P, Flocas HA, Patrikas I, Anagnostopoulou Chr (2001) A 40-year objective
552 climatology of surface cyclones in the Mediterranean region: spatial and temporal
553 distribution. *Int J Climatol* 21: 109–130
554

- 555 Mayengon R (1984) Warm core cyclones in the Mediterranean. *Mar Wea Log* 28: 6–9
556
- 557 Murray RJ, Simmonds I (1991a) A numerical scheme for tracking cyclone centres from
558 digital data. Part I: Development and operation of the scheme. *Aust Meteor Mag* 39: 155–
559 166.
560
- 561 ———, ——— (1991b) A numerical scheme for tracking cyclone centres from digital data. Part
562 II: Application to January and July general circulation model simulations. *Aust Meteor Mag*
563 39: 167–180
564
- 565 Nakicenovic N, Swart R (2000) *IPCC Special Report on Emissions Scenarios*. Cambridge
566 University Press, UK, 570 p
567
- 568 Paciorek CJ, Risbey JS, Ventura V, Rosen RD (2002) Multiple indices of Northern
569 Hemisphere cyclone activity, winters 1949–99. *J Climate* 15: 1573–1590.
570
- 571 Pal JS, Giorgi F, Bi X, Elguindi N, Solmon F, Gao X, Rauscher SA, Francisco R, Zakey A,
572 Winter J, Ashfaq M, Syed FS, Bell JS, Diffenbaugh NS, Karmacharya J, Konare A, Martinez
573 D, Da Rocha RP, Sloan LC, Steiner AL (2007) Regional climate modeling for the
574 developing world: The ICTP RegCM3 and RegCNET. *Bull Amer Meteor Soc* 88: 1395–1409
575
- 576 Pal JS, Small EE, Eltahir EAB (2000) Simulation of regional scale water and energy budgets:
577 Influence of a new moist physics scheme within RegCM. *J Geophys Res* 105: 29 579–29 594
578
- 579 Pezza AB, Simmonds I(2005), The first South Atlantic hurricane: Unprecedented blocking,
580 low shear and climate change. *Geophys Res Lett* 32: L15712, doi:10.1029/2005GL023390.
581
- 582 Picornell MA, Jansa J, Genove A, Campins J (2001), Automated database of mesocyclones
583 from the HIRLAM-0.5 analyses in the western Mediterranean. *Int J Climatol* 21: 335– 354
584
- 585 Pytharoulis I, Craig GC, Ballard SP (2000) The hurricane-like Mediterranean cyclone of
586 January 1995. *Meteorol Appl* 7: 261–279
587
- 588 Reale O, Atlas R (2001) Tropical cyclone-like vortices in the extratropics: Observational
589 evidence and synoptic analysis *Wea Forecast* 16: 7 – 34.
590
- 591 Roeckner E, Bauml G, Bonaventura L, Brokopf R, Esch M, Giorgetta M, Hagemann S,
592 Kirchner I, Kornblueh L, Manzini E, Rhodin A, Schlese U, Schulzweida U, Tompkins A
593 (2003) The atmospheric general circulation model ECHAM5. Part I: Model description. Rep.
594 No. 349, Max-Planck-Institut für Meteorologie, Hamburg, Germany, 127 p
595
- 596 Schepanski K, Knippertz P (2011) Soudano-Saharan depressions and their importance for
597 precipitation and dust: a new perspective on a classical synoptic concept. *Quart J Roy*
598 *Meteorol Soc* 137: 1431-1445
599
- 600 Shapiro LJ (1987) Month-to-month variability of Atlantic tropical circulation and its
601 relationship to tropical cyclone formation. *Mon Wea Rev* 115: 2598–2614
602

- 603 Shapiro MA, Keyser D (1990) Fronts, jet streams and the tropopause. In: Newton CW,
604 Holopainen EO (eds) Extratropical cyclones, The Erik Palmén Memorial Volume, Amer
605 Meteorol Soc, pp 167–191
606
- 607 Simmonds I, Lim E-P (2009) Biases in the calculation of Southern Hemisphere mean
608 baroclinic eddy growth rate. *Geophys Res Letters* 36: L01707, doi:10.1029/2008GL036320
609
- 610 Tous M, Romero R, Ramis C (2010) Medicanes: database and environmental parameters.
611 EGU Abstracts 2010, Vol. 12, EGU2010-12620.
612
- 613 Tous M, Romero R (2011) Medicanes: Criteris de catalogació i exploració dels ambient
614 meteorològics. *Tethys* 8: 53-61
615
- 616 Tous M, Romero R (2012) Meteorological environments associated with medicane
617 development. *Int J Climatol* (in press)
618
- 619 Ulbrich U, Christoph M (1999) A shift in the NAO and increasing storm track activity over
620 Europe due to anthropogenic greenhouse gas. *Clim Dyn* 15:551–559
621
- 622 Uppala, SM, Kållberg PW, Simmons AJ, Andrae U, Bechtold VDC, Fiorino M, Gibson JK,
623 Haseler J, Hernandez A, Kelly GA, Li X, Onogi K, Saarinen S, Sokka N, Allan RP,
624 Andersson E, Arpe K, Balmaseda MA, Beljaars ACM, Berg LVD, Bidlot J, Bormann N,
625 Caires S, Chevallier F, Dethof A, Dragosavac M, Fisher M, Fuentes M, Hagemann S, Hólm
626 E., Hoskins, B. J., Isaksen, L., Janssen, P. A. E. M., Jenne, R., McNally, A. P., Mahfouf, J.-F.,
627 Morcrette J-J, Rayner NA, Saunders RW, Simon P, Sterl A, Trenberth KE, Untch A,
628 Vasiljevic D, Viterbo P, Woollen J (2005) The ERA-40 re-analysis. *Quart J Roy Meteorol*
629 *Soc* 131: 2961–3012
630
- 631 Vallis GK (2006) *Atmospheric and Oceanic Dynamics: Fundamentals and Large-Scale*
632 *Circulation*, Cambridge Univ. Press, New York, 744 p
633
- 634 Walsh KJE, Nguyen K-C, McGregor JL (2004) Fine-resolution regional climate model
635 simulations of the impact of climate change on tropical cyclones near Australia. *Clim Dyn*
636 22: 47-56.
637
- 638 Ziv B, Dayan U, Sharon D (2005) A mid-winter, tropical extreme flood-producing storm in
639 southern Israel: synoptic scale analysis. *Meteorol Atmos Phys* 88: 53-63.

640
641
642
643
644
645
646
647
648
649

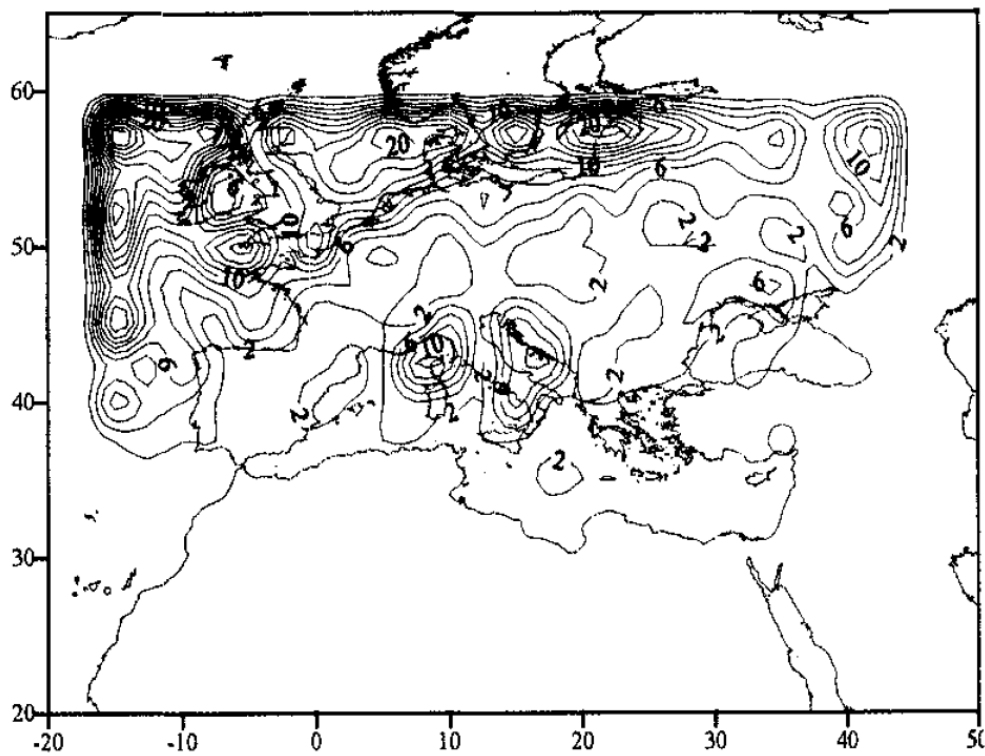


650
651
652

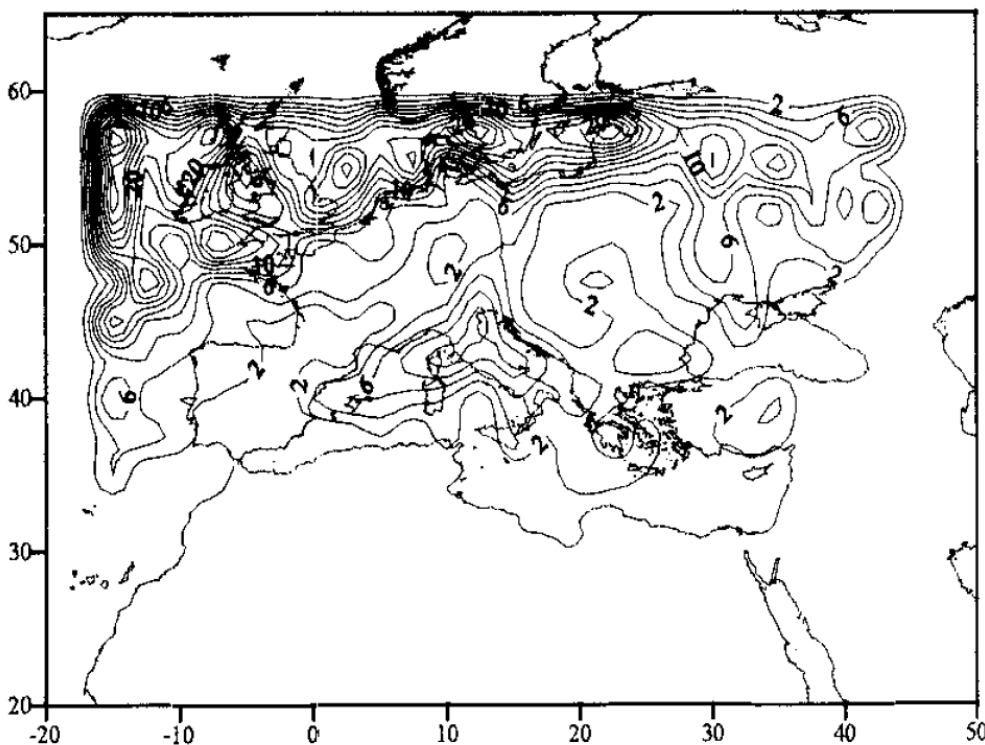
653
654
655
656
657
658
659

Figure 1. Number of warm-core cyclone detections of at least tropical storm strength, per 2x2 degree grid box, for RegCM3 simulation nested within ERA-40 reanalyses, 1981-2000, for each season and the annual totals. Detections are analysed for model output archived four times a day, as described in the text.

660 (a)

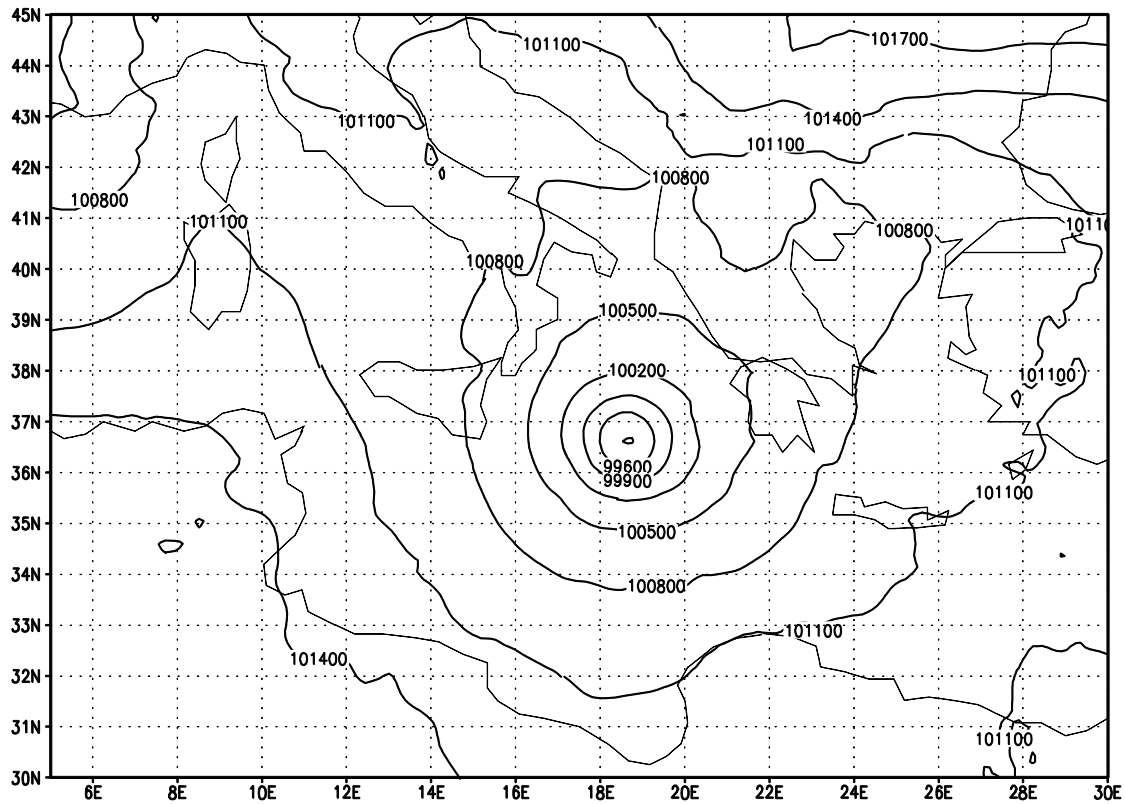


662 (b)



664 Figure 2. Average number of cyclonic disturbances with central pressures less than 995 hPa,
665 per winter season (DJF) per 2.5 degree grid square, for (a) 0000 UTC and (b) 1200 UTC;
666 from Maheras et al. (2001).

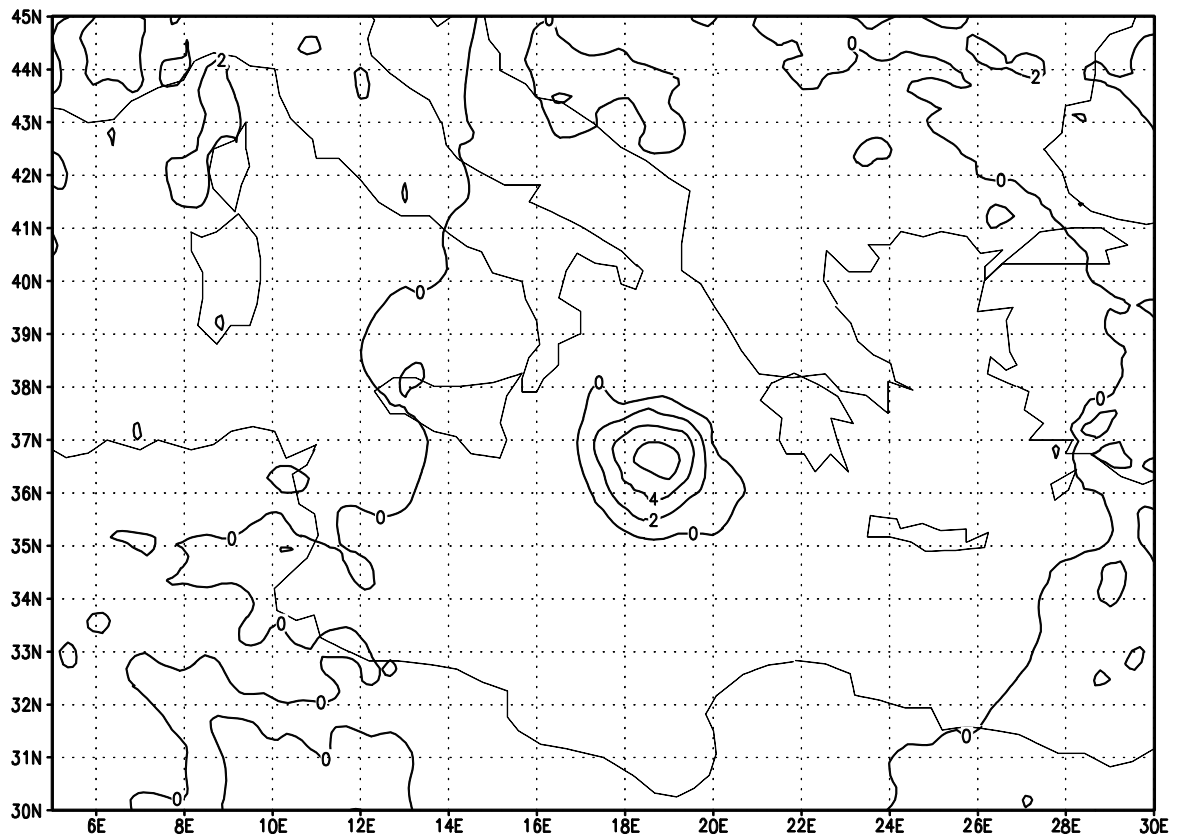
667
668
669
670
671
672



673
674
675
676

Figure 3. Simulated medicane case of 00Z Oct. 23 1994. Contour interval is 300 Pa.

677
678
679



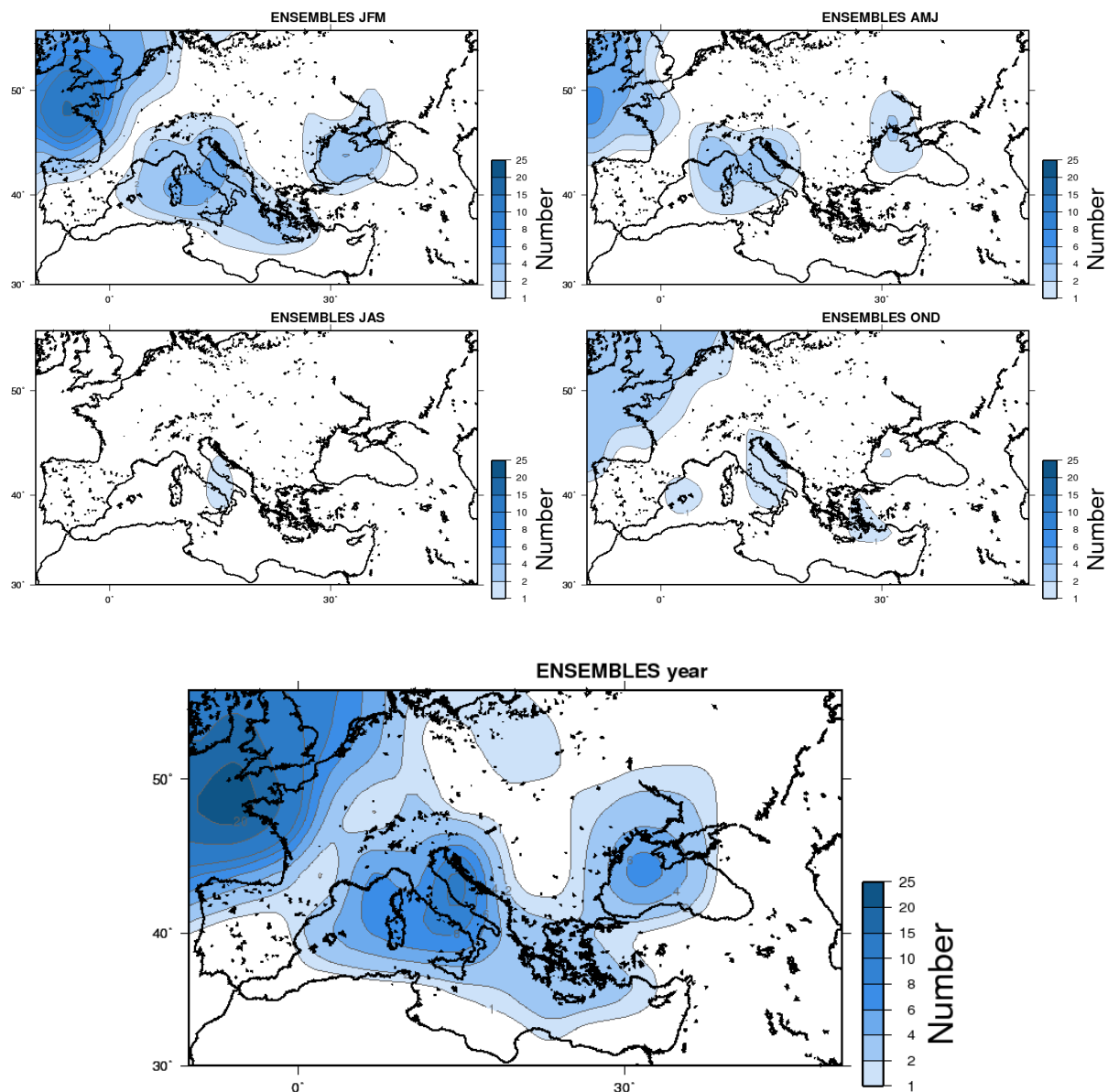
GrADS: COLA/IGES

2011-08-11-13:23

680
681
682
683

Figure 4. The same as Figure 3 but for the sum of the mid-tropospheric temperature anomalies. Contour interval is 2 degrees.

684
685
686
687
688
689
690
691
692
693
694
695
696
697
698

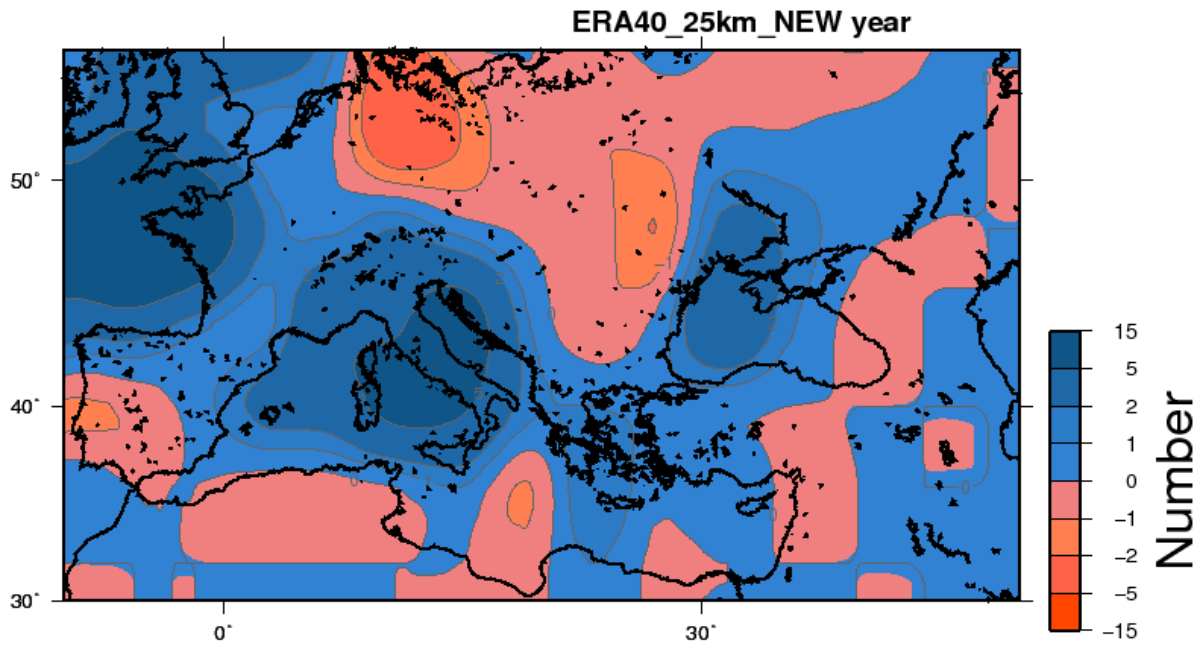


699
700
701

702
703
704
705
706

Figure 5. The same as Fig. 1 except nested within the output of the ECHAM5 GCM, for the seasons indicated.

707
708
709
710
711
712
713
714
715
716

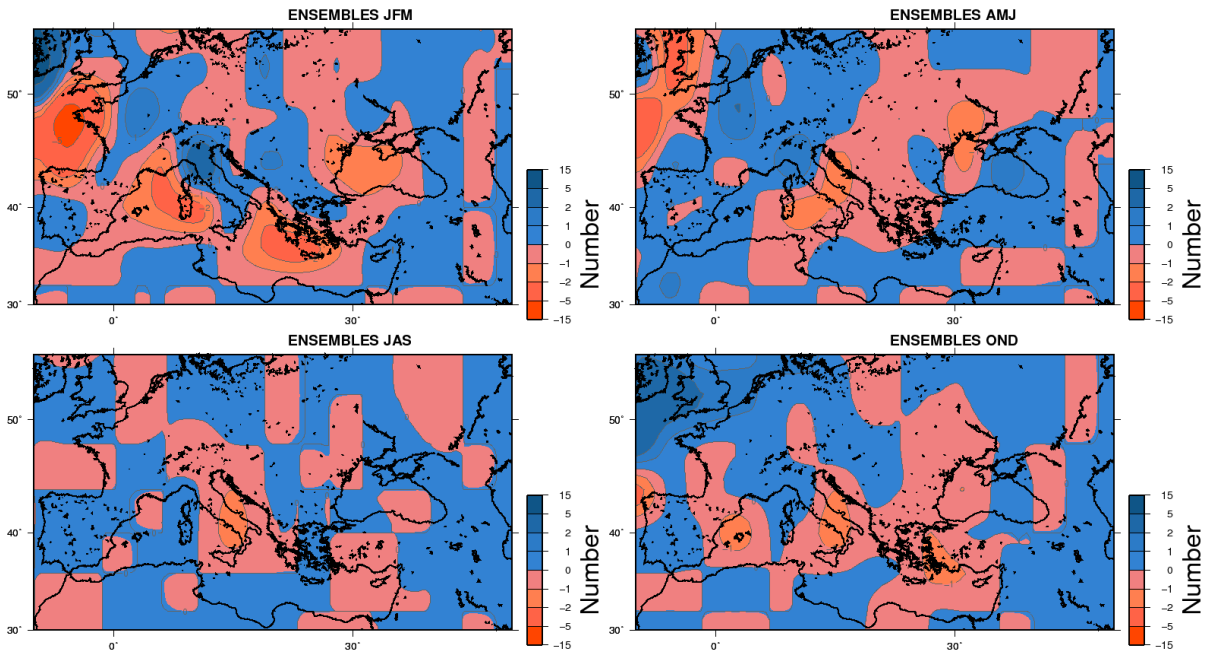


717
718
719
720
721
722
723
724

Figure 6. The same as Fig. 1 except for difference in cyclone occurrence, entire year, ECHAM5-forced run minus ERA-40 forced run.

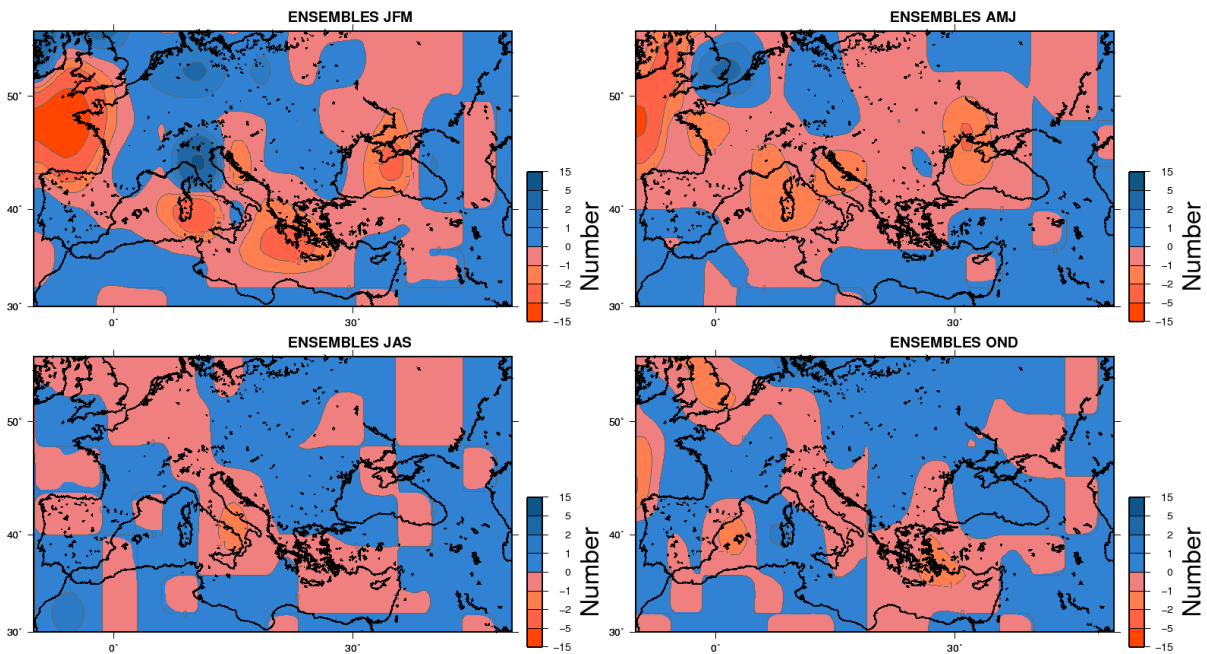
725
726
727
728

(a)



729
730
731

(b)

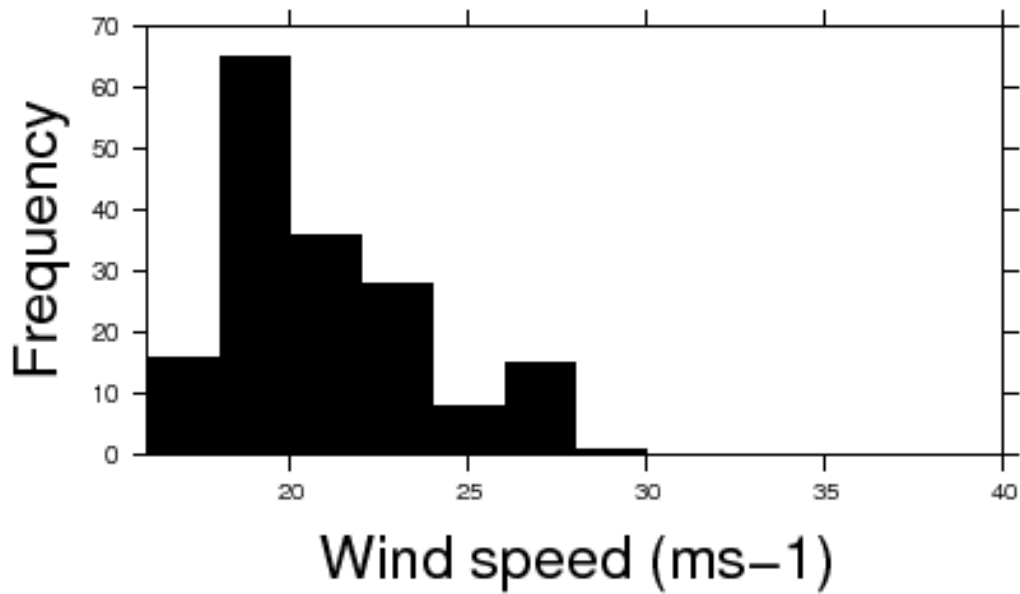


732
733
734
735
736

Figure 7. Differences in numbers of lows between ECHAM5-nested simulations from current-climate simulation, for (a) 2041-2060; and (b) 2081-2100, for each season.

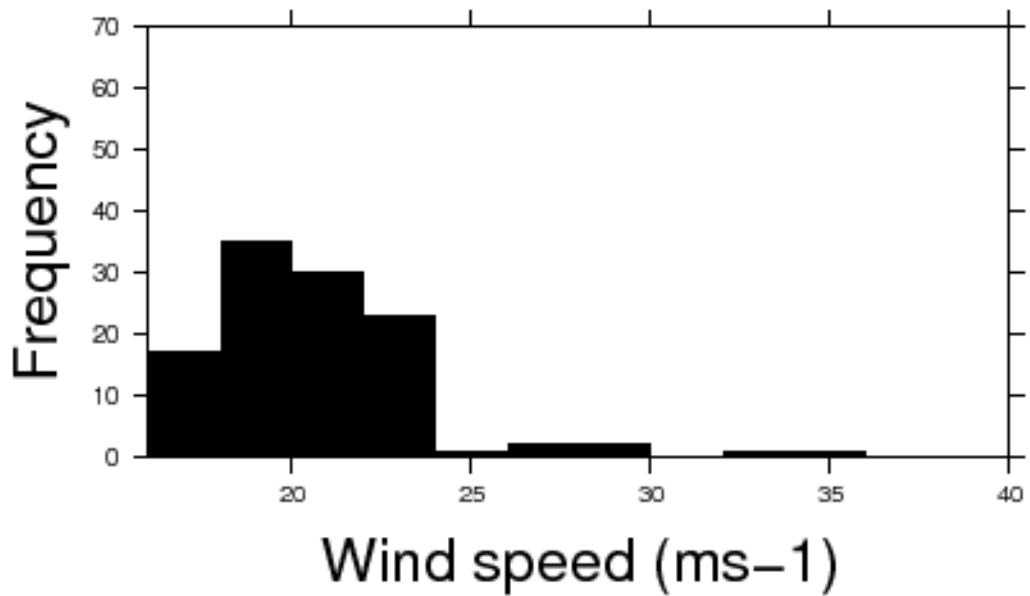
737
738
739
740
741
742
743
744
745
746
747

(a)



748
749
750

(b)

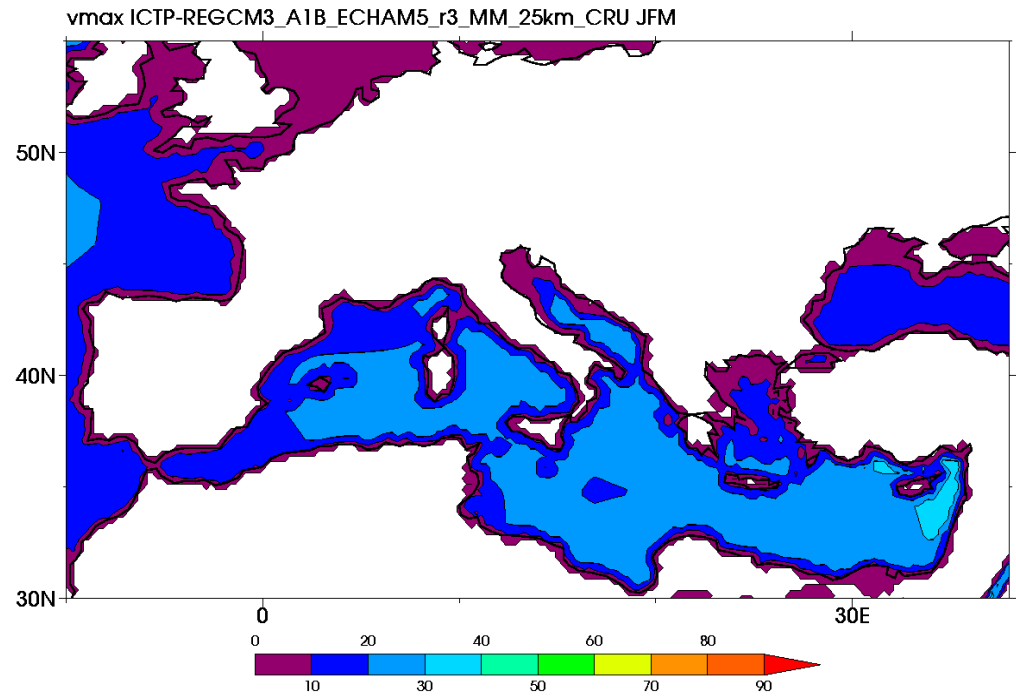


751
752
753
754
755

Figure 8. Histograms of storm maximum wind speed for (a) current climate (1981-2000); and (b) for 2081-2100, with a bin width of 2 ms⁻¹

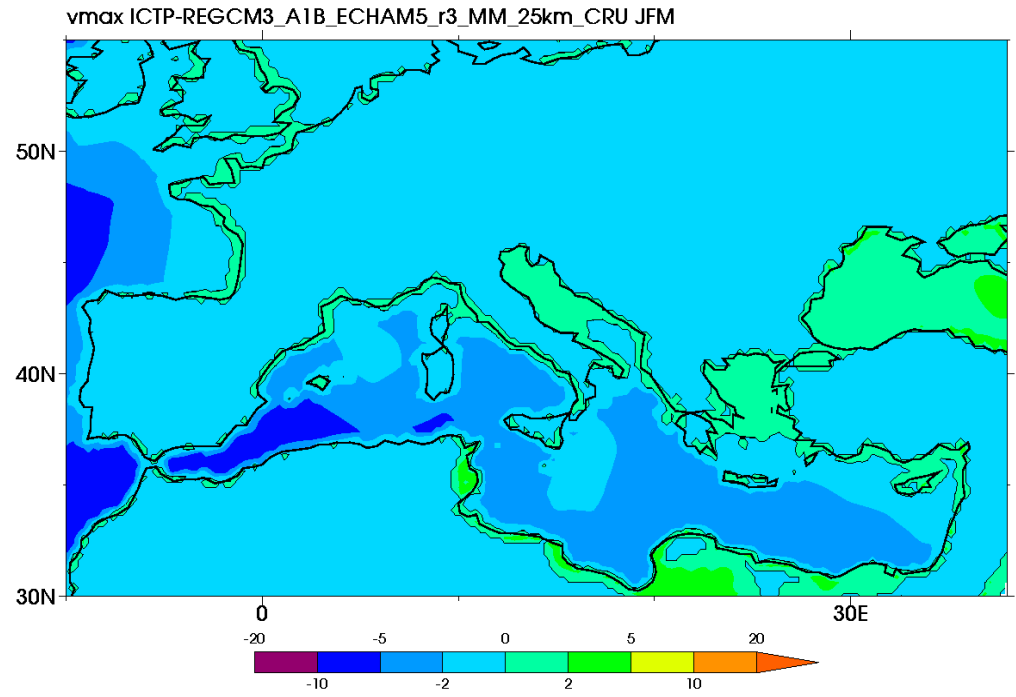
756
757
758
759
760
761

(a)



762
763

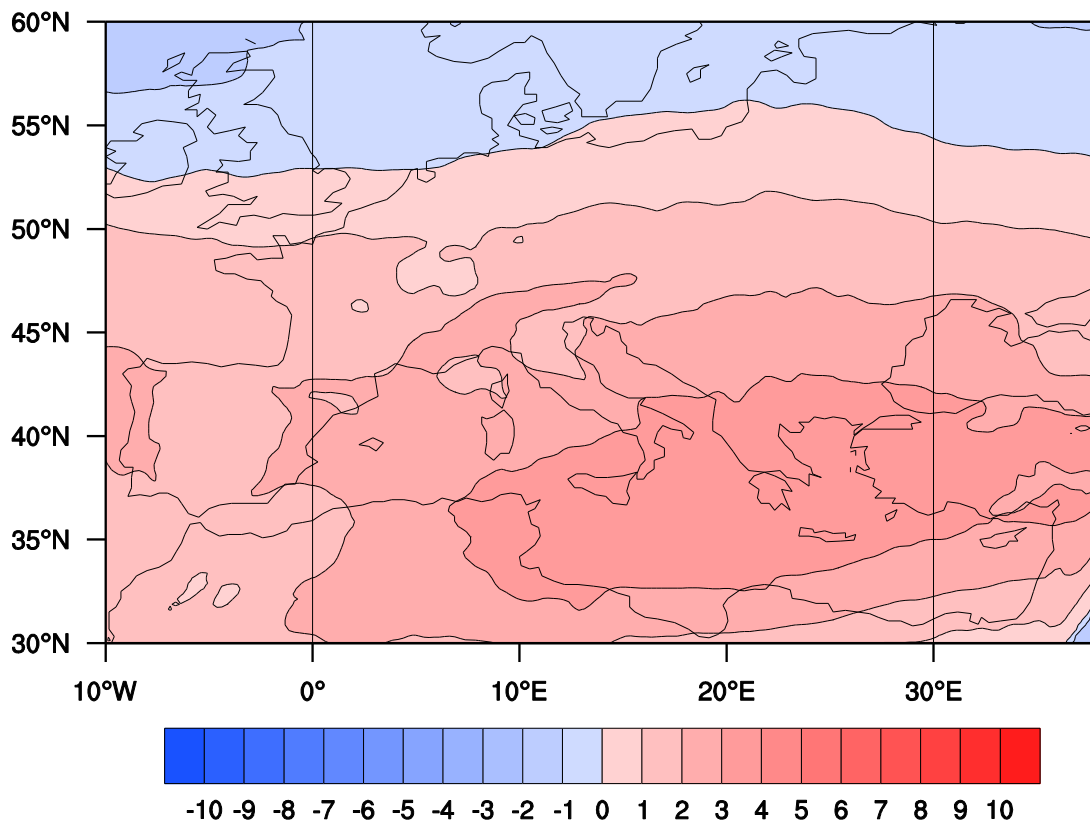
(b)



764
765
766
767
768
769

Figure 9. (a) MPI as expressed by maximum low-level wind speed (V_{max}) for ECHAM5 RegCM3 run, JFM 1981-2000; (b) Difference in V_{max} , 2081-2100 minus 1981-2000, ECHAM5 RegCM3 run.

770
771
772
773
774
775
776
777
778
779

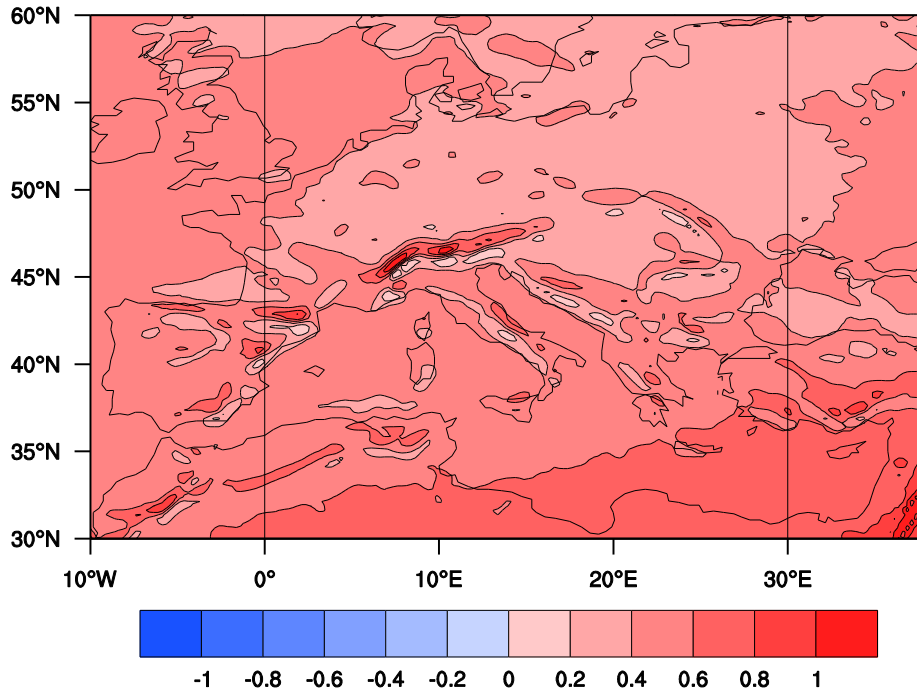


780
781
782
783
784
785

Figure 10. Difference in vertical wind shear, JFM, 2081-2100 minus 1981-2000, ECHAM5 RegCM3 run.

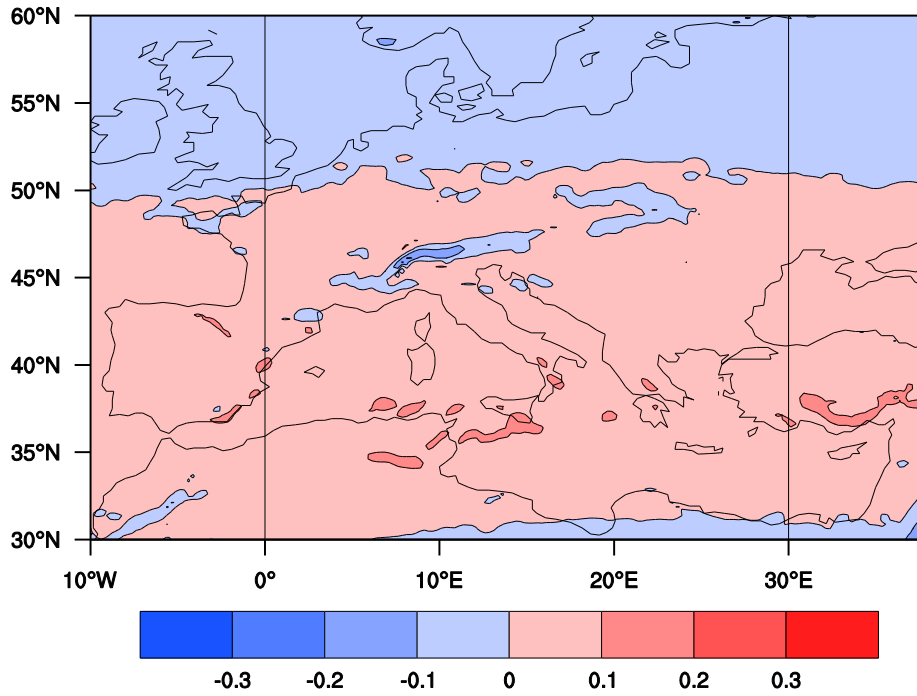
786
787
788
789

(a)



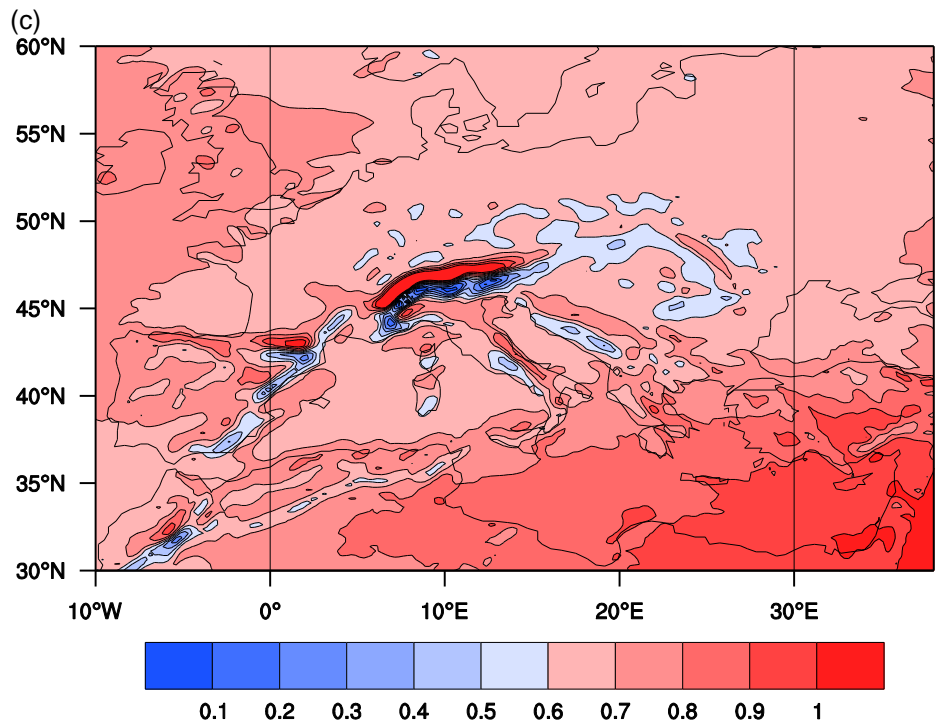
790
791
792
793
794

(b)

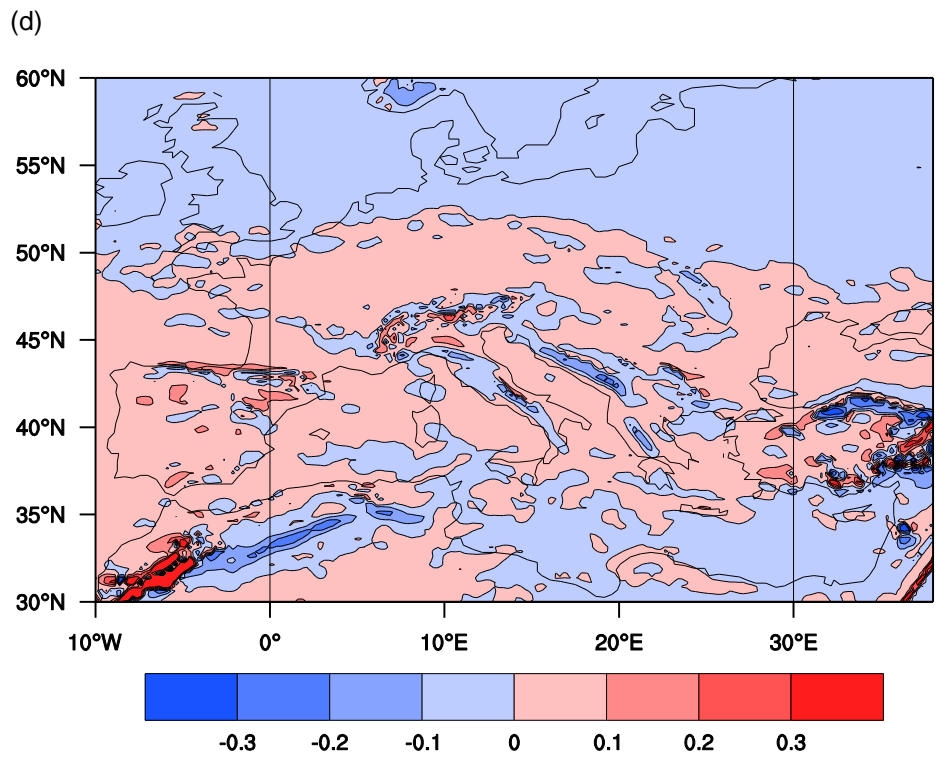


795
796

797



798
799
800
801

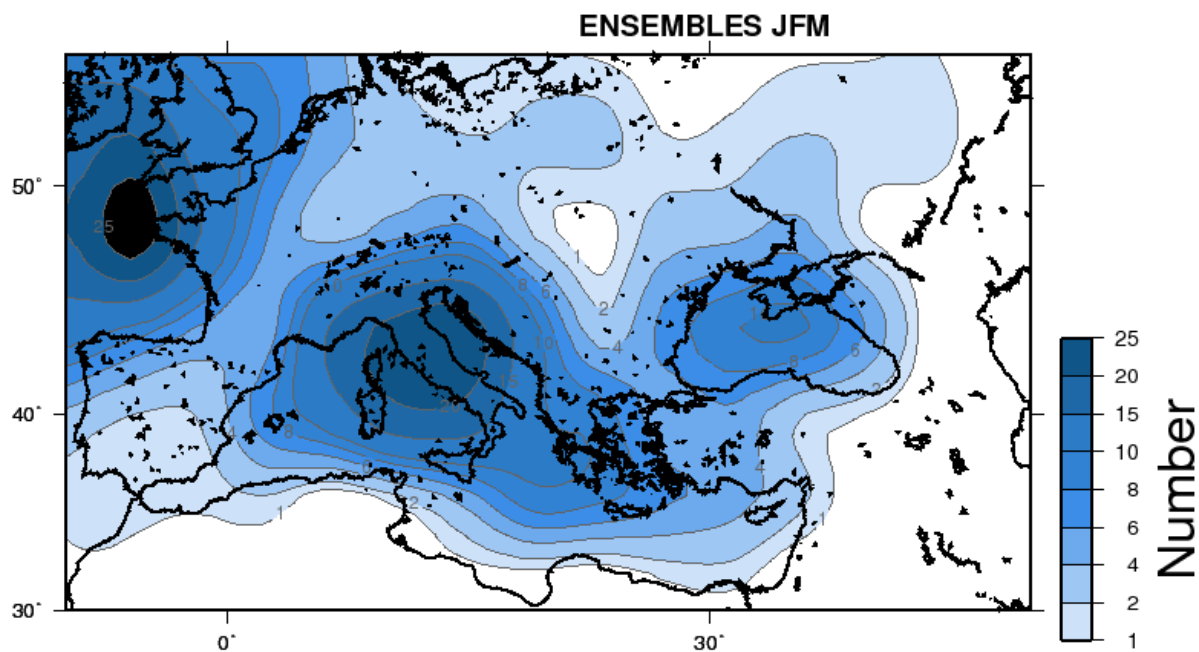


802
803
804
805
806
807
808

Figure 11. (a) JFM current climate 600 hPa EGR; (b) Difference in 600 hPa EGR, 2081-2100 minus 1981-2000; (c) JFM current climate 850 hPa EGR; (d) Difference in 850 hPa EGR, 2081-2100 minus 1981-2000.

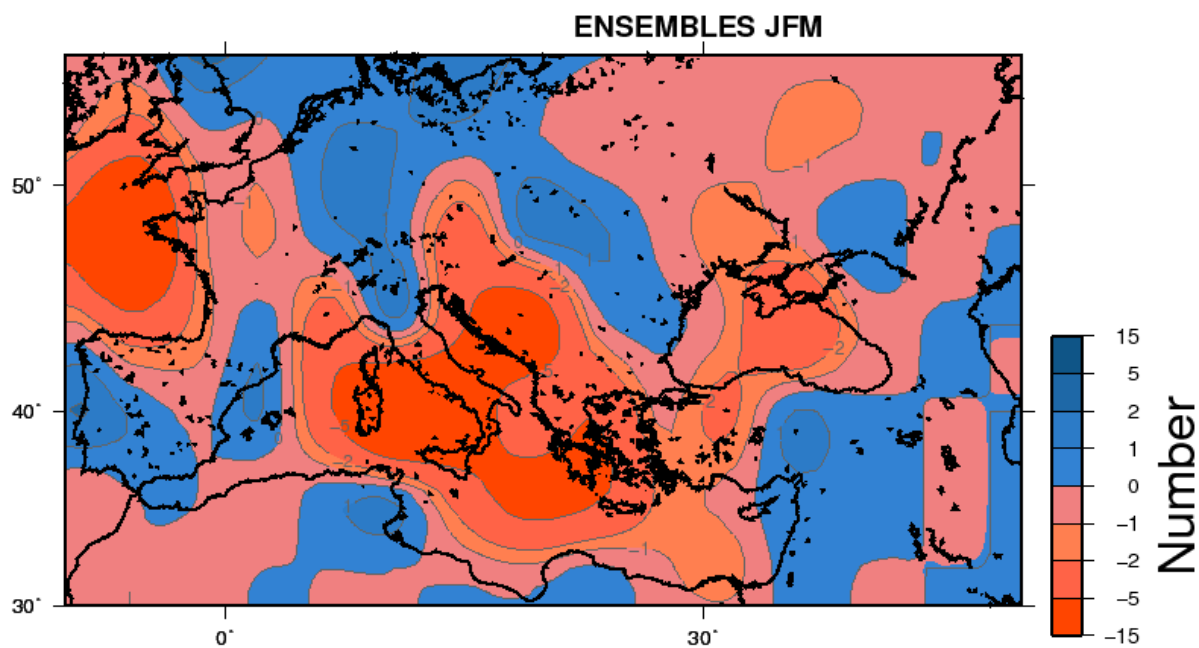
809

810 (a)



811

812 (b)



813

814

815 Figure 12. (a) The same as Fig. 5 (JFM only) but for storms of tropical storm strength that do
816 not satisfy the warm core criteria; (b) the difference for these storms, future minus current
817 climate.